Aqueous-Core Capsules via Interfacial Free Radical Alternating Copolymerization

Dan Wu, Carl Scott, Chia-Chi Ho, and Carlos C. Co*

Department of Chemical and Materials Engineering, University of Cincinnati, Cincinnati, Ohio 45221-0012

Received April 29, 2006; Revised Manuscript Received June 14, 2006

ABSTRACT: Aqueous-core capsules with uniform polymeric shells and diameters ranging from 0.2 to 5 μm were prepared by polymerizing the interfaces of inverse emulsion microspheres. Free-radical polymerization was constrained to the interface of water-in-oil microspheres by the alternating copolymerization of hydrophobic maleate esters and hydrophilic polyhydroxy vinyl ethers, in a manner analogous to classical interfacial polycondensations. In these polymerizations, the kinetics, shell thickness, and release characteristics of the resulting aqueous-core capsules are set by the diffusion-limited alternating reaction of the oil-soluble maleate esters and water-soluble vinyl ethers.

Introduction

Important applications requiring the high-efficiency encapsulation and controlled delivery of drugs, dyes, enzymes, and many other substrates have driven the rapid development of techniques for preparing liquid-core capsules. These varied techniques[1] include polyelectrolyte or colloidal layer-by-layer self-assembly,[2−5] shell polymerization approaches,[1,6] vesicle-based approaches,[7−9] and polymerization in nonsolvents[10] to confine polymerization or assembly of encapsulants at the oil−water interface. Other noteworthy approaches in the recent literature include vapor deposition polymerization on silica and titania nanoparticle surfaces,[11] fabrication of carbon capsules with mesoporous shell structures,[12] pH-responsive capsules,[13] interfacial polycondensation,[14] RAFT polymerizations with miniemulsions[15,16] and polymerization of carboxylic monomers with amine-functionalized biopolymer micelles.[17] This list is by no means comprehensive but illustrates the wide gamut of creative approaches that have been put to bear on the preparation of liquid-core capsules.

In a previous communication,[18] we described a one-step approach for preparing polymer capsules with cores of liquid oil through the alternating free-radical polymerization of hydrophilic vinyl ethers and hydrophobic maleates at the oil−water interface. The low solubilities of the hydrophobic maleate in water and the hydrophilic monomer in oil, coupled with the nature of the alternating copolymerization and reluctance of either monomer to radically homopolymerize constrain the polymerization to the interface. Conceptually, this approach is similar to the interfacial condensation polymerization of hydrophilic diamines and hydrophobic diacid chlorides to form nylon (the popular "nylon rope trick" demonstration). However, unlike interfacial condensation polymerizations, which proceed uncontrollably upon contact of the monomers, this free-radical-based interfacial polymerization allows for thorough emulsification prior to initiation thermally or by UV irradiation.

Having successfully demonstrated the preparation of monodisperse oil-core capsules, we initially thought that aqueous-core capsules could be prepared by starting with a sterically stabilized inverse emulsion prepared using a low HLB surfactant. With the hydrophilic PEG and cationic vinyl ethers used in our earlier report,[18] we explored many combinations of commercially available low-HLB surfactants and steric stabilizers but were unsuccessful in identifying a system that did not phase separate rapidly during the early stages of polymerization. Suspecting that the accumulation of the sterically large PEG units (∼1000 MW) and the electrostatically charged vinyl ethers on the microsphere interface severely destabilized the inverse emulsions, we synthesized a hydrophilic and molecularly compact polyhydroxy vinyl ether (**1**) that copolymerizes with hydrophobic maleates to form aqueous-core capsules. We report here the interesting relationships between polymerization kinetics, structure, and release characteristics of these aqueous-core capsules when prepared under diffusion-limited reaction conditions.

* Corresponding author: Ph (513) 556-2731; Fax (513) 556-3473; e-mail carlos.co@ uc.edu.

Experimental Section

Materials. All reagents and anhydrous solvents were purchased from Sigma-Aldrich or Acros Organics/Fisher Scientific and used without further purification. Reactions were conducted in oven-dried glassware under an argon atmosphere. Poly(ethylene glycol) divinyl ether (MW 240) (**2**), a water-soluble cross-linker, was purchased from Sigma-Aldrich and used as received. Dimethyl 2,2′-azobis(2-methylpropionate) (V601) (**3**), an oil-soluble free radical initiator, was purchased from Wako Chemicals. Dibutyl maleate (**4**) was purchased from Acros Organics and used as received. Span 80 (sorbitan monooleate) was purchased from Sigma-Aldrich and used as received. Hypermer B246SF, a polymeric stabilizer consisting of hydrophobic polyhydroxy fatty acid and hydrophilic poly(ethylene glycol) blocks, was a gift from Uniqema.

Synthesis. 2,3,4,5,6-Pentahydroxy-*N*-[2-(vinyloxy)ethyl]hexanamide (vinyl gluconamide) (**1**) was prepared using a procedure analogous to that of Fuhrop et.[19] Gluconolactone (**5**) (7.6 g, 43 mmol) was suspended in methanol (50 mL) with 2-aminoethyl vinyl ether (**6**) (5 mL, 47 mmol) (Scheme 1). After refluxing for 1 h, the solution became orange color, and upon cooling a white solid precipitated. Following isolation by suction filtration, the solid was recrystallized from methanol to give vinyl ether (**1**) (8.53 g, 32 mmol, 75%) as a while powder; mp = 125−127 °C. ^{1}H NMR (D_2O, 250 MHz) δ: 3.53 (m, 2H), 3.62 (m, 1H), 3.72 (m, 2H), 3.80 (m, 1H), 3.87 (t, J = 5 Hz, 2H), 4.07 (t, J = 3 Hz, 1H), 4.12 (dd, J = 6.2 Hz, 1H), 4.30 (m, 2H), 6.48 (dd, J = 14.6 Hz, 1H). ^{13}C NMR (D_2O, 100 MHz, CH_3OH as standard) δ: 39.0, 63.3, 67.3, 71.0, 71.7, 72.7, 74.0, 88.7, 151.9, 175.1. IR (KBr) cm^{-1}: HRMS

10.1021/ma060951i CCC: $33.50
Published on Web 07/22/2006

Scheme 1. Synthesis of Water-Soluble Vinyl Ether

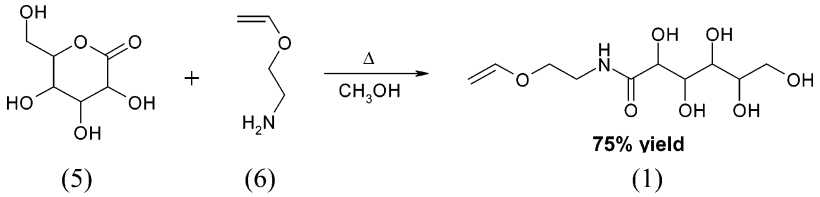

(5) (6) (1)

Scheme 2. Synthesis of Oil-Soluble Cross-Linker

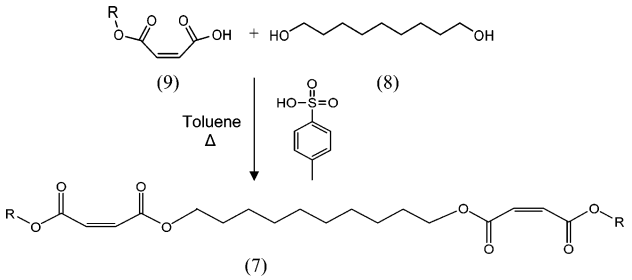

(7)

(ESI, +, polyaniline wash). Calcd for $C_{10}H_{20}O_7N$ (M + 1): 266.1244. Found: 266.1240.

12-{[(2*Z*)]}-4-Butoxy-4-oxobut-2-enoyl]oxy}dodecylbutyl (2*Z*)-but-2-enedioate (**7**) (dimaleate cross-linker): Dodecanediol (**8**) (5.34 g, 26 mmol) and *p*-toluenesulfonic acid (0.49 g, 2.6 mmol) were suspended in toluene (300 mL) and dried by azeotropic distillation. After the distillation of 50 mL of toluene, monobutyl maleate (**9**) (10.3 mL, 59 mmol) was added (Scheme 2). The reaction was heated at reflux for 10 h, during which time toluene was continuously distilled in order to remove the water and methanol produced during the reaction, with the volume of toluene in the flask being kept constant through addition of toluene via an addition funnel. At the completion of the reaction period, toluene was removed by distillation to give a pale brown oil that was taken up in ethyl acetate (100 mL) and extracted with an aqueous sodium bicarbonate solution (3 × 50 mL) to remove excess monomethyl maleate and *p*-toluenesulfonic acid. Following washes with brine (2 × 50 mL), the organic phase was dried over magnesium sulfate. Removal of the solvent gave a brown oil that was diluted with acetone (100 mL) and stored in a freezer for 2 days, causing a white precipitate to fall out of solution. Following filtration to remove the solid (cyclic 1,12-dodecylmaleate) and removal of the solvent by rotary evaporation, the maleate (**7**) was obtained as a pale brown oil (12.84 g, 95%). Cis−trans isomerization of the maleate to the nonpolymerizable fumarate was less than 4%. ^{1}H NMR (CD_2Cl_2, 400 MHz) δ: 0.96 (t, J = 7.4 Hz, 6H), 1.3−1.35 (m, 20H), 1.67 (m, 8H), 4.18 (m, 8H), 6.25 (s, 4H). IR (KBr): 2956, 2928, 2856, 1729, 1644, 1466, 1406, 1376, 1292, 1210, 1163, 983, 814 cm^{-1}.

Interfacial Inverse Emulsion Polymerizations. Inverse emulsions (50 g) were prepared by homogenizing (24 000 rpm IKA-Works T25 Ultra- Turrax) the aqueous and oil phases (20:80 mass ratio), containing the monomers, sodium chloride (osmotic balancing agent to suppress Ostwald ripening), surfactant, and polymeric stabilizer, for 100 min followed by 30 min of horn sonication (278 W, 2.5 s pulses separated by 1 s intervals, Ace Glass Autotune Series 750 W sonicator) in an ice bath. Inverse emulsions were then transferred to an absolute heat flow reaction calorimeter (CPA 200, ChemiSens AB) to monitor the polymerization kinetics. Reactions were initiated thermally at 60 °C via injection of an oil solution of azo-initiator, V601 (0.1 g, 0.43 mmol in 1.0 g decane), through a 1.12 mL injection loop. Kinetic data were collected for 18 h, and the extent of vinyl ether conversion was calculated from the vinyl ether/dibutyl maleate copolymerization enthalpy (61.1 kJ/mol). This enthalpy of copolymerization was calorimetrically measured from the solution polymerizations of equimolar mixtures of ethylene glycol vinyl ether and dibutyl maleate in toluene, whose final conversion was gravimetrically determined.

Polymerization of Dibutyl Maleate (4) and Dimaleate Cross-Linker (7) with Vinyl Gluconamide (1) (Varying Monomer

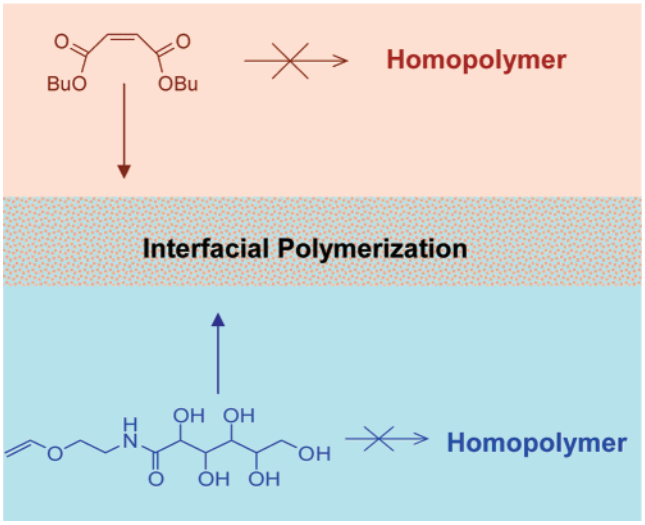

Figure 1. Alternating copolymerization of dibutyl maleate (**4**) and hydrophilic vinyl gluconamide (**1**) initiated with azo-initiator (**3**).

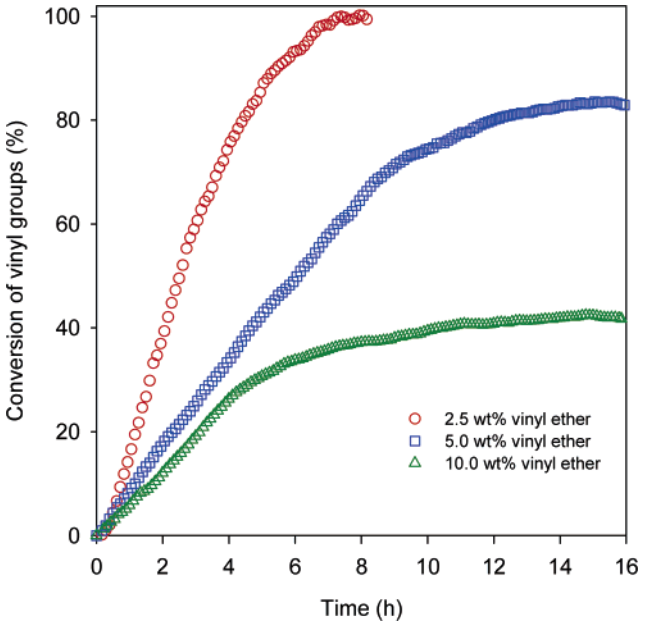

Figure 2. Kinetics of interfacial copolymerization of vinyl gluconamide (**1**) and dibutyl maleate (**4**) for varying loadings of vinyl gluconamide in the aqueous phase. The concentration of maleate monomers in the oil phase is adjusted to maintain an equimolar ratio of maleate to vinyl groups.

Loading; Figure 2). For the 10 wt % vinyl ether sample, the aqueous phase was composed of vinyl gluconamide (**1**) (1.0 g, 3.8 mmol) and 0.1% sodium chloride in water (9.0 g), and the oil phase was composed of dibutyl maleate (0.82 g, 3.6 mmol), dimaleate cross-linker (**7**) (0.043 g, 0.1 mmol), decane (39.1 g), Span 80 (0.75 wt %), and Hypermer B246SF (0.75 wt %). For polymerizations at lower monomer loadings, e.g., 5 and 2.5 wt % vinyl ether, the concentration of maleate monomers was adjusted accordingly to maintain an equimolar ratio of maleate to vinyl double bonds while

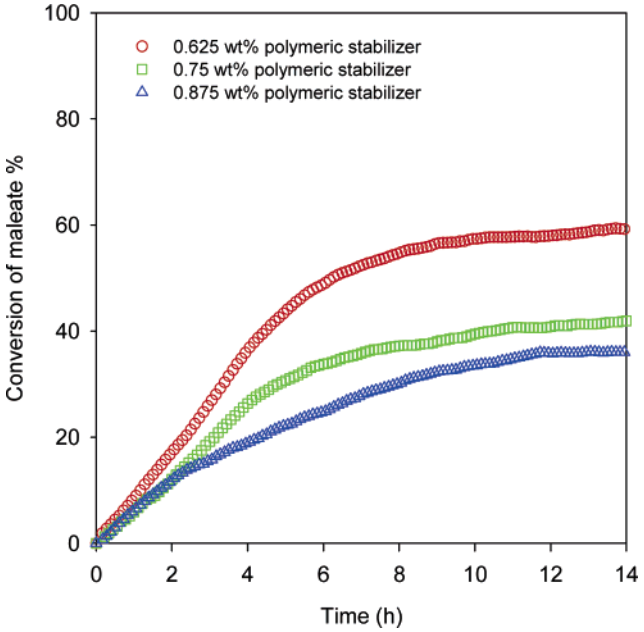

Figure 3. Kinetics of interfacial copolymerization with increasing amount of polymeric stabilizer (Hypermer B246SF).

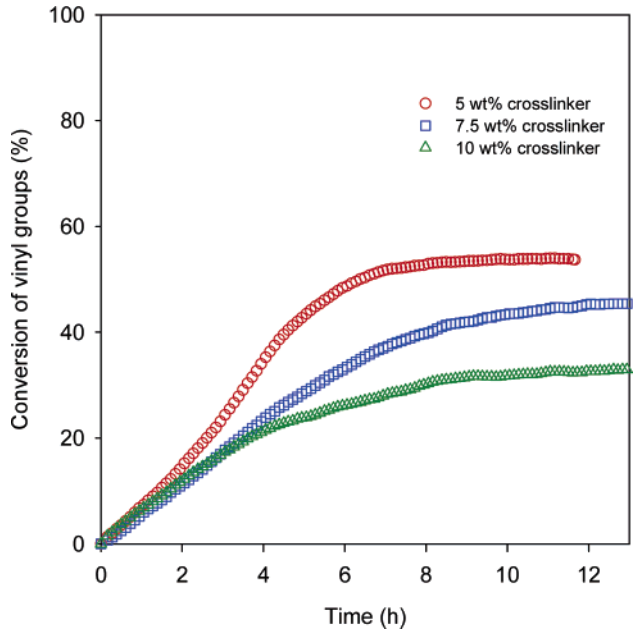

Figure 4. Kinetics of interfacial copolymerization of vinyl gluconamide (**1**) and dibutyl maleate (**4**) following progressive replacement of vinyl gluconamide with PEG divinyl ether (MW 240) cross-linker (**2**). The concentration of dibutyl maleate is adjusted to maintain an equimolar ratio of maleate to vinyl groups.

maintaining the ratio of dimaleate cross-linker to dibutyl maleate fixed at 5 wt %.

Polymerization of Vinyl Gluconamide (1) with Dibutyl Maleate (4) (Varying Loading of PEG Divinyl Ether Cross-Linker (2); Figure 4). For the 5 wt % PEG divinyl ether cross-linker sample, the aqueous phase was composed of vinyl gluconamide (**1**) (0.95 g, 3.6 mmol), PEG divinyl ether (**2**) (0.05 g, 0.2 mmol), and 0.1% sodium chloride in water (9.0 g), and the oil phase was composed of dibutyl maleate (**4**) (0.913 g, 4.0 mmol), decane (39.1 g), Span 80 (0.75 wt %), and Hypermer B246SF (0.75 wt %). For polymerizations at higher cross-linker loadings, e.g., 7.5 and 10 wt % PEG divinyl ether, the corresponding mass fraction of vinyl gluconamide (**1**) is replaced with PEG divinyl ether (**2**) while adjusting the loading of dibutyl maleate (**4**) to maintain an equimolar ratio of maleate to vinyl double bonds.

Polymerization of vinyl gluconamide (**1**) and 5 wt % PEG divinyl ether cross-linker (**2**) with maleates of varying hydrophobicity. Aqueous phase: vinyl gluconamide (**1**) (0.95 g, 3.6 mmol), PEG divinyl ether (**2**) (0.05 g, 0.2 mmol), 0.1% sodium chloride in water (9.0 g). Oil phase: diethyl (**10**), dibutyl (**4**), or dioctyl maleate (**11**) (4.0 mmol), decane (39.0 g), Span 80 (0.75 wt %), and Hypermer B246SF (0.75 wt %).

Monomer Partition Coefficients. To measure the partition coefficient of the different maleates monomers under reaction conditions, aqueous mixtures containing 10% vinyl gluconamide (**1**) were thoroughly mixed at 60°C for 3 h with decane containing an equimolar loading of maleate at an aqueous to oil phase mass ratio of 20:80. The concentrations of the individual maleates in the aqueous phase were measured by UV spectroscopy (λ_{max} = 230−235 nm, Cary 50 Bio, Varian). The concentration of maleate remaining in the oil phase was calculated by mass balance. For vinyl gluconamide (**1**), the partition coefficient was measured by ^{1}H NMR (400 MHz) replacing H_2O with D_2O.

Characterization. TEM images were obtained using a JEOL JEM-1230 transmission electron microscope equipped with an AMT Advantage Plus 2K × 2K digital camera. One drop of sample was diluted 100× with hexanes, placed on a copper grid coated with 100 mesh Formvar (Electron Microscopy Sciences), blotted gently with filter paper to a thin film spanning the grid, and dried under vacuum for 2 days at room temperature prior to imaging. No contrast agents were applied.

For confocal imaging, 0.01% Rhodamine B (Fisher Scientific) was dissolved into the aqueous phase prior to the reaction. Images were acquired using a Zeiss LSM 510 laser scanning confocal microscope and analyzed using the LSM software. One drop of sample was diluted 100× with hexanes, placed on a glass cover slide, and air-dried at room temperature prior to imaging.

Encapsulation and release characteristics of the capsules were measured by adding 0.01% Rhodamine B to the aqueous phase prior to the reaction. After polymerization, samples were placed in a glass vial and air-dried to remove the organic solvent. After redispersion in water, the samples were transferred into dialysis tubes (molecular weight cutoff 60 kDa) (Fisher Scientific) and immersed in 100 mL of water at room temperature. At periodic intervals, 2 mL samples were withdrawn from external aqueous phase, and the amount of dye released was determined by fluorescence. Control samples containing Rhodamine B solutions of the same concentration were directly loaded into the dialysis tubes without encapsulation to evaluate the mass transfer resistance of the dialysis tubing. Encapsulation and release experiments were performed in triplicate for each sample.

Results and Discussion

Polymerization Kinetics. Owing to the low solubilities of vinyl gluconamide in the oil phase and dibutyl maleate in the aqueous phase, the polymerizations are constrained to proceed at the oil−water interface due to the alternating nature of the copolymerization and the reluctance of either monomer to radically homopolymerize. As the polymer shell forms, monomer diffuses to the interface, and the position of highest radical activity within the polymerizing interface is presumably set by the relative diffusion rates of the hydrophobic and hydrophilic monomers to the active radical ends. We thus studied the inverse emulsion polymerization kinetics, varying the concentrations of monomer, polymeric stabilizer, and cross-linker to identify signatures of a diffusion limited reaction. In these studies, vinyl gluconamide (**1**) and dibutyl maleate (**4**) are fractionally replaced with cross-linking PEG divinyl ethers (**2**) or dimaleates (**7**) to form robust capsules. In all cases, the molar ratio of vinyl to maleate groups is equimolar to allow, in principle, 100% conversion. We also confirmed that no polymerization occurs when either the vinyl ether or maleate monomer is absent.

As shown in Figure 2, the rate of polymerization and the ultimate conversion are strongly dependent on the amount of

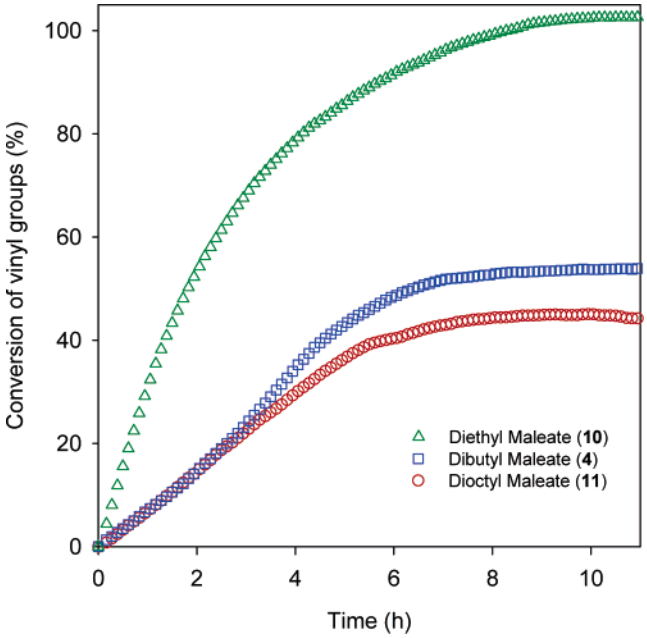

Figure 5. Kinetics of interfacial copolymerization of vinyl gluconamide (**1**) with maleates of increasing hydrophobicity.

monomer. Increasing the vinyl ether loading in the aqueous phase from 2.5% to 5% and 10%, while adjusting the maleate loading to maintain equimolar conditions, depresses the ultimate conversion from ~100% to ~80% and ~40%, respectively. Assuming that the microsphere size distribution is not affected by the monomer concentration, increasing the monomer loading would result in thicker shells and, presumably, a greater barrier to diffusion for the same degree of conversion. The observed reduction in the ultimate conversion with increasing monomer loading suggests strongly that the reaction can be limited by the diffusion of monomers into the polymerizing shell.

In addition to the polymeric shell that results from the interfacial copolymerization, we found that the commercial block copolymer (Hypermer B246SF) used to sterically stabilize the drops also hinders the reaction. As shown in Figure 3, increased loadings of the polymeric stabilizer reduces significantly the ultimate conversion. Introduction of cross-linkers, which should yield a denser polymerizing interface with lower permeability, could also reduce the ultimate conversion. We verified this experimentally as shown in Figure 4, where progressive replacement of vinyl gluconamide (**1**) with a cross-linker, PEG divinyl ether (MW 240) (**4**), results in a clear reduction in ultimate conversion.

The basic premise of this approach to confining radical polymerization at oil−water interfaces lies in the alternating copolymerization of hydrophobic and hydrophilic monomers that do not homopolymerize. In the idealized case where the hydrophobic and hydrophilic monomers partition exclusively in the oil and aqueous phase, respectively, polymerization would proceed only at the oil/water interface. After the oil/water interface is covered with polymer, further polymerization would be severely retarded even if the polymerized interface is partially swollen with water or oil. In practice, where the monomers cross-partition between aqueous and oil phases, the polymerization takes place over a finite interfacial region that extends into both water and oil phases. Should both monomers be water-soluble, an extreme example of cross-partitioning, the reaction would occur principally in the aqueous core, yielding solid porous particles with little to no diffusive barriers to polymerization.

To study the effect of monomer cross-partitioning, we examined the polymerization kinetics of vinyl gluconamide (**1**) with dioctyl (**11**), dibutyl (**4**), and diethyl (**10**) maleates, fixing the maleate loading at 4 mmol and equimolar to vinyl gluconamide in each case. Under polymerization conditions at 60 °C, the water−oil partition coefficient (C_{water}/C_{oil}) of this series of maleates increases from 0.078 (dioctyl), 0.086 (dibutyl), to 0.14 (diethyl). As Figure 5 shows, changing the partitioning of the monomer has a significant effect on the polymerization kinetics. While the polymerization with diethyl maleate reaches ~100% in ~10 h, the polymerization with dibutyl maleate and dioctyl maleate reach their ultimate conversion of only ~52% and ~42%, respectively, following ~6 h. The increased partitioning of diethyl maleate in the aqueous phase likely results in a broader zone of polymerization that extends further into the aqueous phase, resulting in thicker shells compared to that for dibutyl maleate and dioctyl maleate. Under these conditions, the oil−water partition coefficient (C_{oil}/C_{water}) of vinyl glucon-

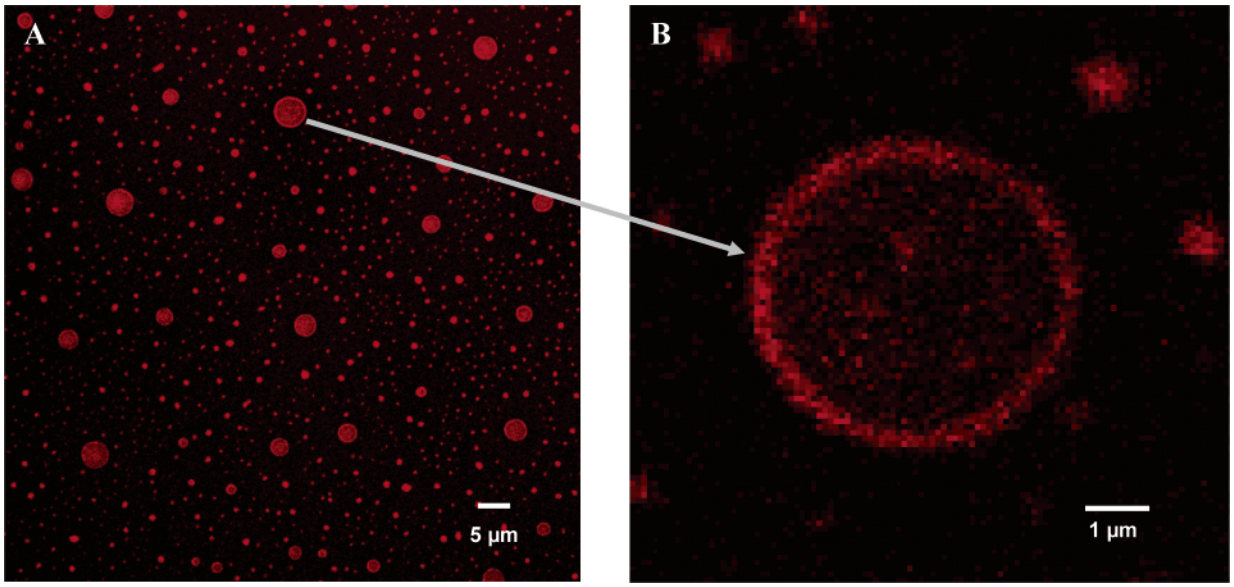

Figure 6. (A) Fluorescence image of dehydrated aqueous-core capsules. (B) Confocal image of the horizontal cross section of the particle shown by the arrow.

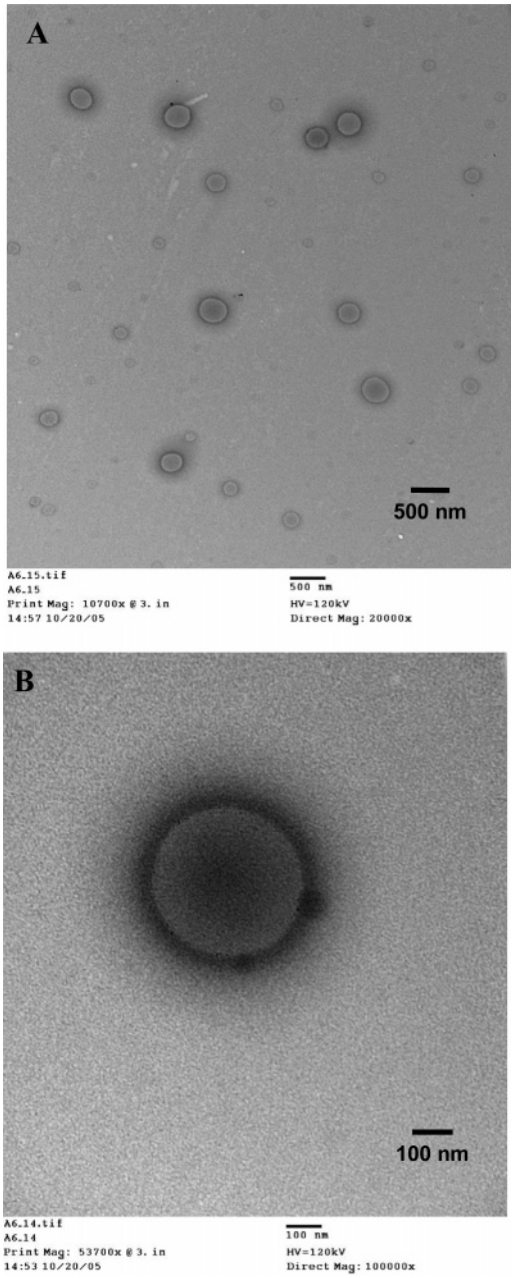

Figure 7. TEM image of submicron aqueous-core capsules.

amide is only ~0.016, and we expect its contribution toward broadening the zone of polymerization is not only constant but also small compared to that of the maleates.

Capsule Structure. To visualize the polymerized capsules, we added a water-soluble dye, Rhodamine B, into the aqueous phase and polymerized the sample under the conditions of Figure 4 with 5 wt % PEG divinyl ether cross-linker. As the capsules dry, Rhodamine B partitions into the polymer shell as shown in the fluorescence and confocal images (Figure 6). Although the starting inverse emulsion does not contain any micron-size drops, following polymerization, the size distribution of the capsules is clearly bimodal, with a few micrometer capsules present in a population of mostly submicron capsules. It is likely that interfacial polymerization partially destabilizes the droplets during early stages of polymerization, causing coalescence, which results in the larger capsules. For the micrometer-size capsules, confocal cross-sectional imaging (Figure 6B) confirms the presence of a well-defined polymer shell into which Rhodamine B precipitates following drying of the oil and

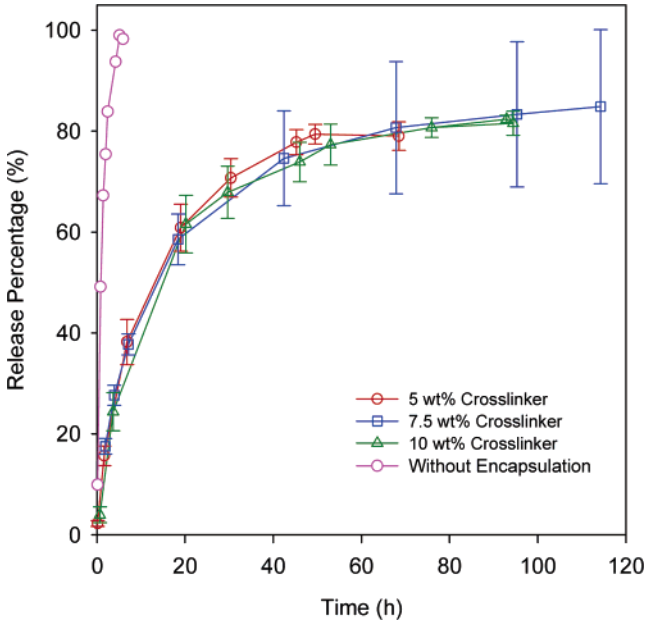

Figure 8. Release profiles of Rhodamine B. The percentage of released Rhodamine B was calculated relative to the initial amount of Rhodamine B loading inside the aqueous-core capsules.

aqueous phases. For the submicron population of capsules, transmission electron microscopy confirms the presence of a defined polymer shell structure (Figure 7A,B). Because misfocused TEM images of solid particles can also appear to have a core−shell structure, we carefully adjusted the focus in both limits and verified that no focusing adjustment yields a solid structure.

While the capsule size distribution exhibits a bimodal distribution, the shells of individual capsules are uniform as shown in the confocal and TEM images. Moreover, polymer-bridged capsules were not observed despite the relatively high volume fraction (~20%) of the capsules. The uniformity of the capsule shells and the absence of bridging likely come from the diffusion-controlled nature of the interfacial polymerization. Because neither monomer homopolymerizes, both monomers must diffuse into the polymerizing shell to meet and react. With the locus of polymerization within the polymerizing shells themselves, the shells must grow thicker from the inside out. Polymerization in the continuous oil phase, which could lead to bridging of multiple microspheres, is thus unlikely. Within one capsule, thicker shell regions grow more slowly compared to thinner regions where transport of monomer to the growing radical chains occurs more rapidly. This self-regulating mechanism is a possible explanation for the uniformity in shell thickness of individual capsules.

Encapsulation and Release. To investigate the encapsulation and release properties of the aqueous-core capsules, Rhodamine B was added to the aqueous phase prior to emulsification and interfacial polymerization. After polymerization the capsules are evaporated of oil then rehydrated into a water-continuous phase to study their release characteristics (the cross-linked polymer shells remain intact during this process). Figure 8 shows the release characteristics of three capsules prepared with 5, 7.5, and 10 wt % cross-linker corresponding to the kinetic curves shown in Figure 4. Compared to the control sample without encapsulation, which releases all of its Rhodamine B over ~3 h, the polymerized capsules exhibit progressive release over a ~40 h period.

It is initially puzzling to observe almost identical release characteristics for the three capsule systems with different

degrees of cross-linking. However, this can be understood by considering that diffusion of the monomers sets the ultimate conversion during polymerization and cross-linking reduces both (Figure 4). Irrespective of the cross-linker loading, the shells of the capsules polymerize to a thickness limited by the diffusion of the monomers. Capsules prepared with more cross-linker are likely thinner than those prepared with less cross-linker, and their permeabilities are balanced exactly by the diffusion-limited polymerization.

Conclusions

The polymerization kinetics, structure, and release characteristics of aqueous-core capsules prepared via free-radical alternating copolymerization of hydrophilic vinyl ethers and hydrophobic alkyl maleates at the interface of water-in-oil microspheres have been studied. The polymerization kinetics and ultimate conversion are generally limited by the diffusion of monomer into the polymerizing shell, and full conversion of monomers occurs only at low monomer loadings or in cases when monomers with significant cross-partitioning in both aqueous and oil phases are used. While this diffusion-limited polymerization leads to capsules with uniform shells, it also restricts the maximum shell thickness and sets a minimum bound on the permeability of the capsules.

Acknowledgment. We thank Birgit Ehmer and Nancy Klenne for assistance with the TEM and confocal imaging and the National Science Foundation (CTS#0324303) and American Chemical Society Petroleum Research Fund for financial support of this work.

References and Notes

(1) Meier, W. *Chem. Soc. Rev.* **2000**, *29*, 295−303.
(2) Caruso, F.; Caruso, R. A.; Mohwald, H. *Science* **1998,** *282*, 1111−1114.
(3) Dinsmore, A. D.; Hsu, M. F.; Nikolaides, M. G.; Marquez, M.; Bausch, A. R.; Weitz, D. A. *Science* **2002,** *298*, 1006−1009.
(4) Shchukin, D. G.; Sukhorukov, G. B. *Adv. Mater.* **2004,** *16*, 671−682.
(5) Velev, O. D.; Furusawa, K.; Nagayama, K. *Langmuir* **1996,** *12*, 2374−2384.
(6) Wendland, M. S.; Zimmerman, S. C. *J. Am. Chem. Soc.* **1999,** *121*, 1389−1390.
(7) Jung, M.; Hubert, D. H. W.; van Veldhoven, E.; Frederik, P.; van Herk, A. M.; German, A. L. *Langmuir* **2000**, *16*, 3165−3174.
(8) Krafft, M. P.; Schieldknecht, L.; Marie, P.; Giulieri, F.; Schmutz, M.; Poulain, N.; Nakache, E. *Langmuir* **2001**, *17*, 2872−2877.
(9) McKelvey, C. A.; Kaler, E. W.; Zasadzinski, J. A.; Coldren, B.; Jung, H. T. *Langmuir* **2000**, *16*, 8285−8290.
(10) McDonald, C. J.; Bouck, K. J.; Chaput, A. B.; Stevens, C. J. *Macromolecules* **2000**, *33*, 1593−1605.
(11) Jang, J.; Lee, K. *Chem. Commun.* **2002**, 1098−1099.
(12) Yoon, S. B.; Sohn, K.; Kim, J. Y.; Shin, C. H.; Yu, J. S.; Hyeon, T. *Adv. Mater.* **2002**, *14*, 19−21.
(13) Duan, H. W.; Kuang, M.; Zhang, G.; Wang, D. Y.; Kurth, D. G.; Mohwald, H. *Langmuir* **2005**, *21*, 11495−11499.
(14) Torini, L.; Argillier, J. F.; Zydowicz, N. *Macromolecules* **2005**, *38*, 3225−3236.
(15) Luo, Y. W.; Gu, H. Y. *Macromol. Rapid Commun.* **2006**, *27*, 21−25.
(16) van Zyl, A. J. P.; Bosch, R. F. P.; McLeary, J. B.; Sanderson, R. D.; Klumperman, B. *Polymer* **2005**, *46*, 3607−3615.
(17) Hu, Y.; Jiang, X. Q.; Ding, Y.; Chen, Q.; Yang, C. Z. *Adv. Mater.* **2004**, *16*, 933−937.
(18) Scott, C.; Wu, D.; Ho, C. C.; Co, C. C. *J. Am. Chem. Soc.* **2005**, *127*, 4160−4161.
(19) Fuhrhop, J. H.; Boettcher, C. *J. Am. Chem. Soc.* **1990**, *112*, 1768−1776.

MA060951I